Numerical Simulation of the Turbulent Flow over a three-Dimensional Flat Roof

M. Raciti Castelli, A. Castelli, E. Benini

Abstract—The flow field over a flat roof model building has been numerically investigated in order to determine three-dimensional CFD guidelines for the calculation of the turbulent flow over a structure immersed in an atmospheric boundary layer. To this purpose, a complete validation campaign has been performed through a systematic comparison of numerical simulations with wind tunnel experimental data.

Wind tunnel measurements and numerical predictions have been compared for five different vertical positions, respectively from the upstream leading edge to the downstream bottom edge of the analyzed model. Flow field characteristics in the neighborhood of the building model have been numerically investigated, allowing a quantification of the capabilities of the CFD code to predict the flow separation and the extension of the recirculation regions.

The proposed calculations have allowed the development of a preliminary procedure to be used as guidance in selecting the appropriate grid configuration and corresponding turbulence model for the prediction of the flow field over a three-dimensional roof architecture dominated by flow separation.

Keywords—CFD, roof, building, wind

I. INTRODUCTION AND BACKGROUND

WIND loads on the roof of a civil structure inside an industrial area still represent a great challenge for structural engineers. The quantitative amounts of force and pressure coefficients depend on the shape, size and orientation of the building and on its interaction with the surrounding environment. The flow around buildings is still extremely difficult to predict by computational methods, even for simple surrounding environments [1].

As focused by Krishna et al. [2], wind causes a random time-dependent load, which can be considered as a mean plus a fluctuating component. Strictly speaking, all civil structures experience dynamic oscillations due to the fluctuating component (gustiness) of wind, however, in short rigid structures, such oscillations are insignificant and the buildings can therefore be satisfactorily treated as being subjected to an equivalent static pressure. This approach is taken by most Codes and Standards. However, the response of a civil structure to high wind pressure depends not only on the geographical location and proximity of other obstructions to airflow, but also on the characteristics of the structure itself.

Marco Raciti Castelli is a Research Associate at the Department of Mechanical Engineering of the University of Padua, Via Venezia 1, 35131 Padova, Italy (e-mail: marco.raciticastelli@unipd.it).

Alberto Castelli has completed his M.Sc. in Mechanical Engineering at the Department of Mechanical Engineering of the University of Padua, Via Venezia 1, 35131 Padova, Italy.

Ernesto Benini is an Associate Professor at the Department of Mechanical Engineering of the University of Padua, Via Venezia 1, 35131 Padova, Italy (e-mail: ernesto.benini@unipd.it).

As a matter of fact, most buildings present "bluff forms" to the wind, making it difficult to ascertain the wind forces accurately. Thus, the problem of bluff-body aerodynamics remains largely in the empirical/descriptive realm of knowledge. Furthermore, the flow patterns (and hence the wind pressures/forces) change with the Reynolds number, making the direct application of wind tunnel test results to real structures quite difficult [3]. Nevertheless, the limitations in accurate aerodynamic databases can be overcome by using advanced Computational Fluid Dynamics (CFD) codes, which can outflank the lack of experimental data thanks to their inherent ability to determine the aerodynamic components of actions through the integration of the Navier-Stokes equations.

Performing CFD calculations can provide knowledge about the flow-field around the building in all its details, such as velocities, pressures, etc. Moreover, all types of useful graphical presentations, such as flow lines, contour lines and iso-lines are readily available. As suggested by Jensen et al. [4], this stage can be considered as if an accurate wind-tunnel study or an elaborate full-scale measurement campaign had been conducted. Nevertheless, several questions relating to the quality and trust of the numerical predictions come along with the use of such tools [5]. In fact, despite its widespread use, the prediction accuracy and many factors that might affect simulation results are not yet thoroughly understood [6] and, as reported by Franke et al. [7], the general appraisal of the computational approach for quantitative (and sometimes even qualitative) predictions is expressed as lack of confidence. Many emerging issues - concerning wind loadings on civil engineering structures under extreme weather conditions, pedestrian comfort, optimal conditions for wind turbines, ventilation and dispersion inside urban areas - still remain to be solved. As a matter of fact, as pointed out by Stathopoulos [8], the flow around buildings is still extremely difficult to predict by computational methods, even for simple surrounding environments.

However, the testing of scale models in a boundary layer wind tunnel, capable of simulating the main velocity profile and turbulence of the natural wind, has been shown to be a very effective method of prediction by comparison with respective full-scale data. This sort of considerations led to the idea of performing numerical validation tests against experimental atmospheric wind tunnel measurements, in order to clarify ambiguities and develop some practical guidelines for CFD predictions of wind flows around buildings by assessing the influence of various computational variables, such as grid resolution, boundary conditions and turbulence models. A selection of the work of Ozmen et al. [9] was chosen as the reference benchmark for the numerical modeling of the wind flow around a simple rectangular building characterized by a flat roof.

In order to develop a preliminary procedure to be used as a guidance in selecting the appropriate grid configuration and corresponding turbulence model for the prediction of the flow field over a two-dimensional roof architecture dominated by flow separation, Raciti Castelli et al. recently tested the capability of several turbulence models to predict the separation that occurs in the upstream sector of the roof and the extension of the relative recirculation region for different vertical longitudinal positions, respectively from the upstream leading edge to the downstream bottom edge of a reference model building [10]. Also spatial node distribution was investigated, in order to determine the best compromise between numerical prediction accuracy and computational effort. The validation work proved *Standard k-ε* turbulence model to be quite accurate in predicting the flow-features, especially after the recirculation region in the upstream portion of the building. On the basis of this preliminary study, the present work investigates the potential of the numerical code in reproducing the turbulent flow over a three-dimensional flat roof model building. Wind tunnel measurements and numerical predictions have been compared for five different vertical positions, respectively from the upstream leading edge to the downstream bottom edge of the analyzed model, allowing a quantification of the capabilities of the CFD code to predict the flow separation and the extension of the recirculation regions.

II. THE CASE STUDY

The proposed numerical simulations were based upon the measurements performed by Ozmen et al. [9] in the VKI (von Karman Institute) L-2B wind tunnel [11] by using a 1:100 scale model of the BBRI experimental building [12]: by means of the Counihan technique [13], a turbulent boundary layer of 150 mm thickness was reproduced, allowing the experimental investigation of the flow patterns over the building model.
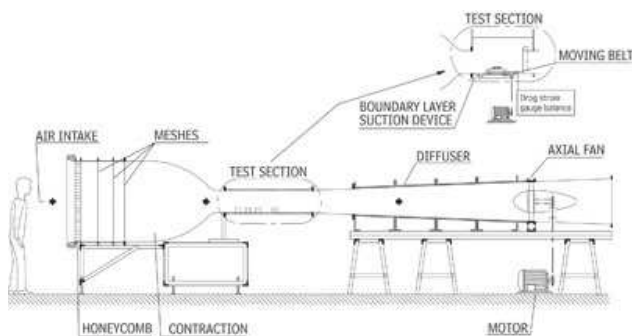

Fig. 1 Schema of the L-2B facility at VKI (from: [14])

The L-2B facility is a low speed, open circuit wind tunnel of the suction type. It incorporates an air inlet, fitted with honeycomb and meshes, a two-dimensional contraction and several interchangeable test sections of 0.35 m height, 0.35 m width and various lengths from 0.9 m to 2 m, as can be seen from Fig. 1.

III. MODEL GEOMETRY

In the present work, the flow field inside the wind tunnel was numerically simulated by reproducing a computational domain of square section, having the same wind tunnel test section size. Table I, Figs. 2 and 3 summarize the main scale model and test section dimensions.

TABLE I
MAIN SCALE MODEL AND TEST SECTION DIMENSIONS

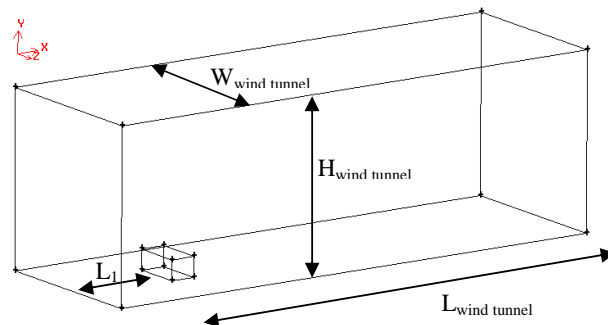| Denomination	Value [m]
$H_{wind\ tunnel}$ [mm]	350
$L_{wind\ tunnel}$ [mm]	1050
$W_{wind\ tunnel}$ [mm]	350
L_1 [mm]	200
H [mm]	40
L [mm]	50
W [mm]	100
δ [mm]	150
δ/H [-]	3.75

Fig. 2 Main dimensions of the overall computational domain
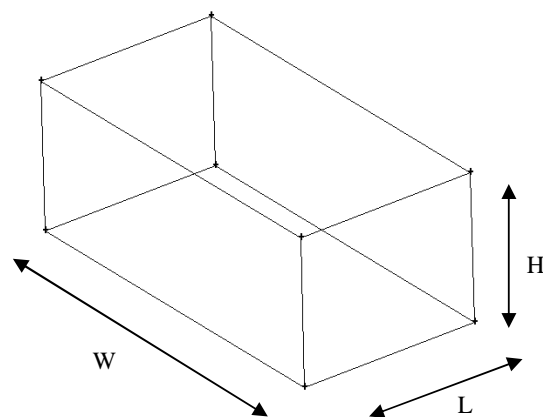

Fig. 3 Main dimensions of the model building

The numerical model boundary conditions are represented in Fig. 4. Both *Wall* and *Symmetry* boundary conditions were adopted for the upper and side portions of the computational domain, and their influence on the numerical results proved completely negligible.
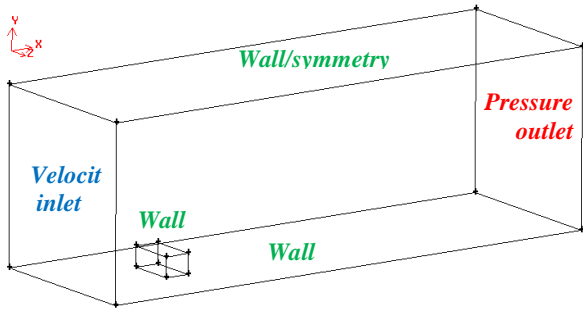
Fig. 4 Boundary conditions of the computational model

Through the use of proper User Defined Functions (UDFs), the same profiles of the reference boundary layer (in terms of both mean velocity and turbulence intensity) obtained by Ozmen et al. [9] were reproduced in the numerical simulations, as can be seen from Figs. 4 and 5, reporting respectively the mean horizontal velocity profile normalized with respect to the reference velocity along the horizontal axis (assumed 15 m/s) and the boundary layer turbulence intensity profile, defined as:

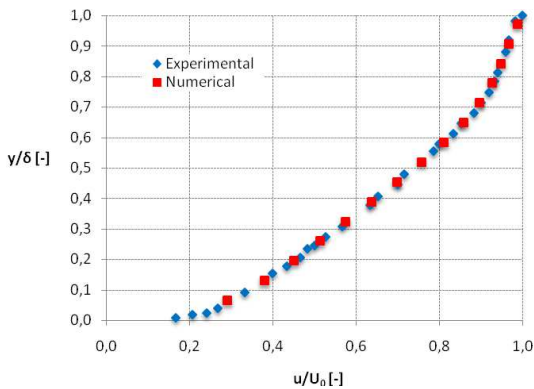$$I(y) = u'/U_0 \tag{1}$$

where

$$u' = (u'^2_x)^{0.5} \tag{2}$$

Fig. 5 Comparison between the boundary layer mean horizontal velocity profile obtained by Ozmen et al. [9] and the one adopted in the proposed numerical calculations (the mean horizontal velocity profile was normalized with respect to the reference velocity along the horizontal axis, assumed 15 m/s)

The validation procedure was performed through the comparison of numerical and experimental measurements of the vertical profiles of the x-component mean velocity at five reference positions along the roof length. Fig. 7 shows the displacement of the reference positions, whose normalized x-coordinates with respect to the model building height, defined as:

$$\bar{x} = \frac{x_{reference\ position}}{H} \tag{3}$$
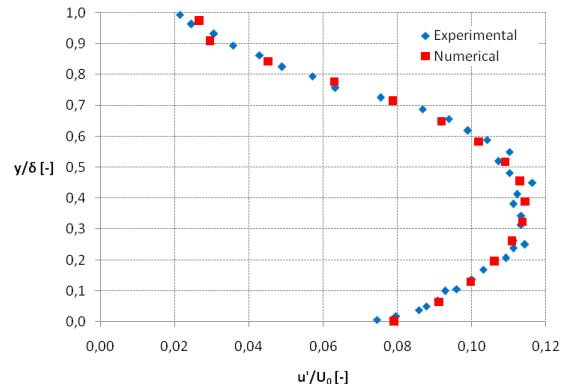
are reported in Table II.

Fig. 6 Comparison between the boundary layer turbulence intensity profile obtained by Ozmen et al. [9] and the one adopted in the proposed numerical calculations
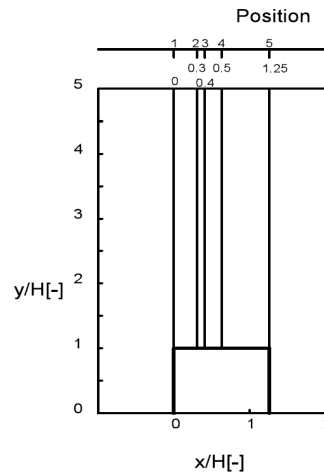

Fig. 7 Displacement of the five reference positions along the roof length that were used for the validation procedure

TABLE II
NORMALIZED X-COORDINATES OF THE FIVE REFERENCE POSITIONS WITH RESPECT TO THE MODEL BUILDING HEIGHT (THE ORIGIN OF THE COORDINATE REFERENCE SYSTEM IS LOCATED AT THE MODEL BUILDING UPSTREAM LEADING EDGE)

Reference position No.	$\bar{x}$ $[-]$
1	0.00
2	0.30
3	0.40
4	0.50
5	1.25

IV. SPATIAL DOMAIN DISCRETIZATION

An isotropic unstructured mesh was created around the model building, in order to test the prediction capability of a very simple grid. Considering their features of flexibility and adaption capability, unstructured meshes are in fact very easy to obtain, for complex geometries, too, and often represent the "first attempt" in order to get a quick response from the CFD in engineering work.

Raciti Castelli et al. [10] investigated the sensitivity to grid resolution for the flat roof case adopting five different mesh architectures, named *Model_0*, *Model_1*, *Model_2*, *Model_3* and *Model_4*. In Table 3 the characteristic data of the tested grid configurations are reported, as a function of the normalized grid resolution on the model building, defined as:

$$\text{Res}_{model} = \Delta g_{model}/H \qquad (4)$$

and as a function of the normalized grid resolution on outer computational domain, defined as:

$$\text{Res}_{domain} = \Delta g_{domain}/H \qquad (5)$$

TABLE III
CHARACTERISTIC DATA OF THE TESTED GRID CONFIGURATIONS

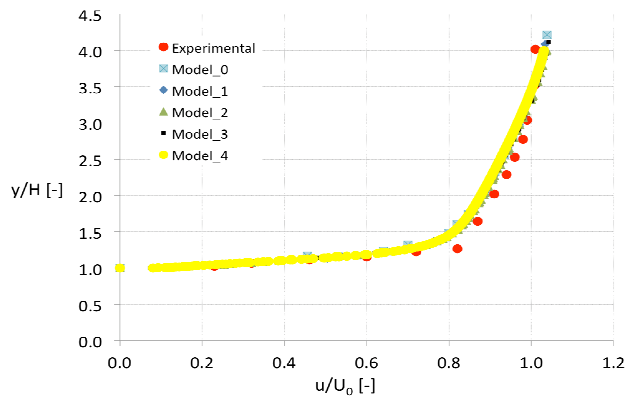| Grid name	Res_{model} [-]	Growth factor [-]	Red_{domain} [-]
Model_0	0.2500	1.1	2.500
Model_1	0.1250	1.1	0.250
Model_2	0.0250	1.1	0.250
Model_3	0.0025	1.1	0.250
Model_4	0.0025	1.1	0.025

Fig. 8 Comparison between measured and computed x-velocity profiles as a function of grid resolution, *Standard k-ε* turbulence model, reference position No. 3 (from: [10])

As can be seen from Fig 8, showing the comparison between measured and numerically simulated x-velocity profiles as a function of grid resolution for the reference position No. 3, the effect of grid resolution on the computed x-velocity profiles is entirely negligible, being the very same results obtained by the coarser mesh and the finer one. *Model_2* mesh was adopted for numerical calculations.

Figs. 9 and 10 show a comparison of the main geometrical features of *Model_0*, *Model_2* and *Model_4* grid refinements near the model building, while Fig. 10 displays the whole *Model_2* mesh.
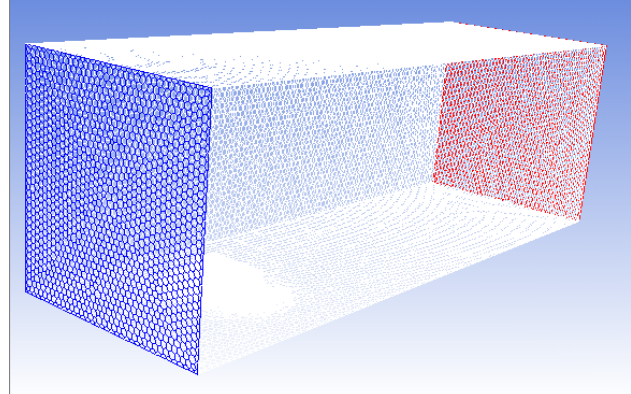

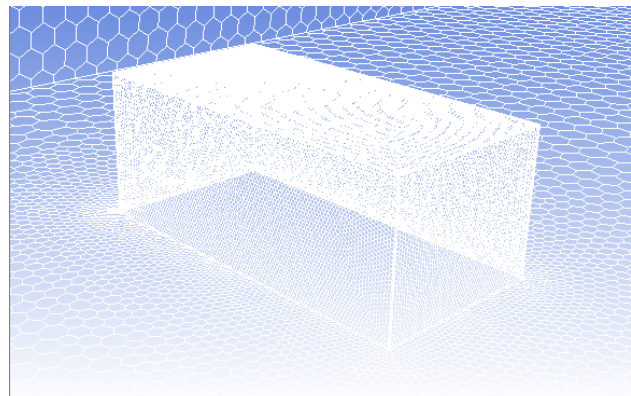Fig. 9 Main geometrical features of *computational domain mesh*

Fig. 10 Main geometrical features of the grid refinement near the model building

V. TURBULENCE MODELS AND CONVERGENCE CRITERIA

Simulations were performed using the commercial RANS solver ANSYS FLUENT®, which implements 3-D Reynolds-averaged Navier-Stokes equations using a finite volume-finite element based solver. A segregated solver, implicit formulation, was chosen for unsteady flow computation. The fluid was assumed to be incompressible, being the maximum fluid velocity on the order of 16 m/s. As far as the turbulence model is concerned, *Standard k-ε* was adopted for viscous computations.

As a global convergence criterion, residuals were set to 10^{-5}. Each simulation, performed on a 2.33 GHz clock frequency quad core CPU with Hyper-Threading, required a total computational time of about 5 hours.

VI. RESULTS AND DISCUSSION

Figs. from 11 to 15 represent the comparison between measured and numerically simulated x-velocity profiles for the five reference positions along the roof length.
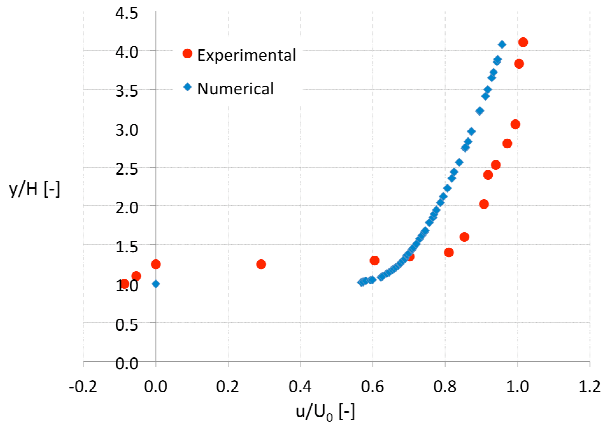
Fig. 11 Comparison between measured and computed x-velocity profiles, reference position N° 1
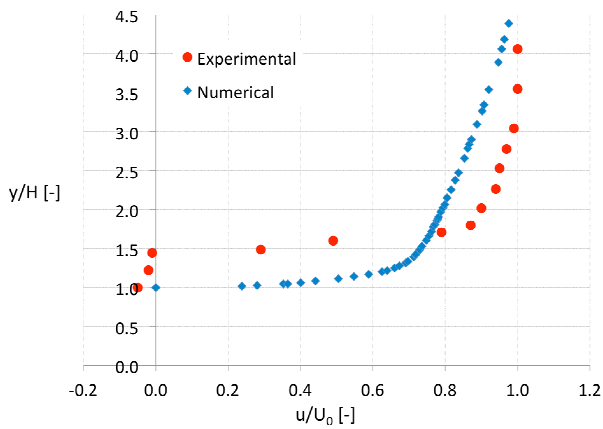

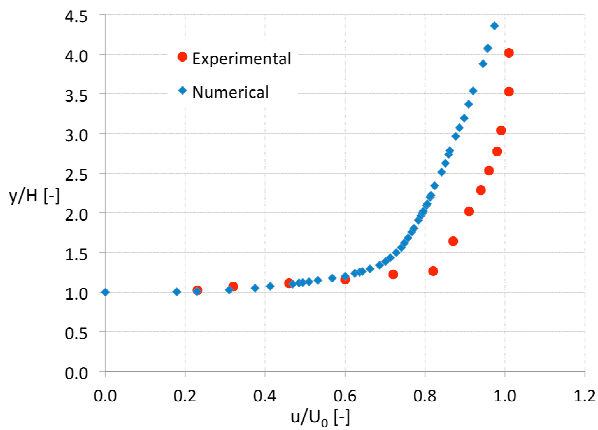Fig. 12 Comparison between measured and computed x-velocity profiles, reference position N° 2

Fig. 13 Comparison between measured and computed x-velocity profiles, reference position N° 3

The following observations can be drawn:

1. the numerical code proved to be accurate in predicting the main features of the flow field near the building model;

2. the accuracy in the prediction of the main flow field characteristics lowers close to the model roof, especially for reference positions No. 1 and 2, that is as the flow separates from the upstream leading edge of the building model;

3. the numerical code proved to be accurate in predicting the flow-field features close to the model building for reference positions No. 3, 4 and 5, that is after the recirculation region in the upper portion of the model roof;

4. small discrepancies are registered between measured and computed velocity values for y/H higher than 1.5; further work is required in order to better investigate this phenomenon.
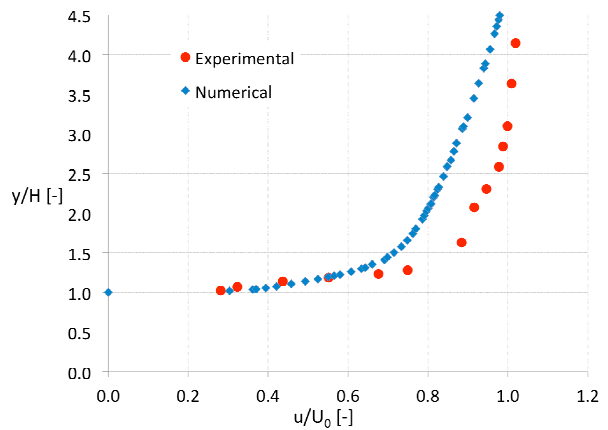

Fig. 14 Comparison between measured and computed x-velocity profiles, reference position N° 4
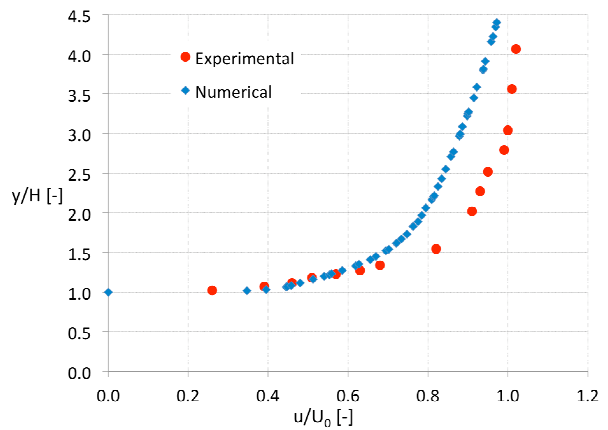

Fig. 15 Comparison between measured and computed x-velocity profiles, reference position N° 5

Fig. 16 represents the contours of absolute velocity on five bounded planes at the top of the roof and parallel to the unperturbed flow direction. A small reduction in the separation bubble on top of the roof, passing from the central (evidenced by the red arrow) to the side sections (evidenced by the blue arrows) is clearly visible.

This phenomenon is connected to the tip effects at the building sides, as can be seen also from Figs. 17 and 18, showing a comparison between measured and computed pathlines around the model building. Good agreement can be registered between experimental flow visualization and the CFD simulation, being the numerical code able to correctly reproduce the two symmetrical downwind vertical structures (evidenced by the red circles), as well as flow separation at side walls (evidenced by the yellow circles).
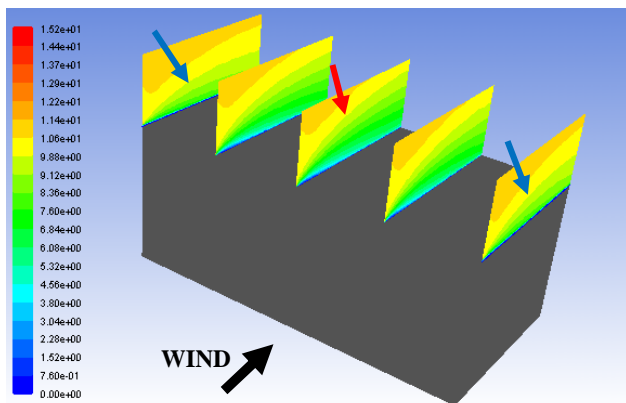

Fig. 16 Contours of absolute velocity [m/s] on five bounded planes at the top of the roof and parallel to the unperturbed flow direction. The red arrow evidences flow separation in the central building section, while the blue arrows evidence reduced flow separation in the side building section, due to tip effects
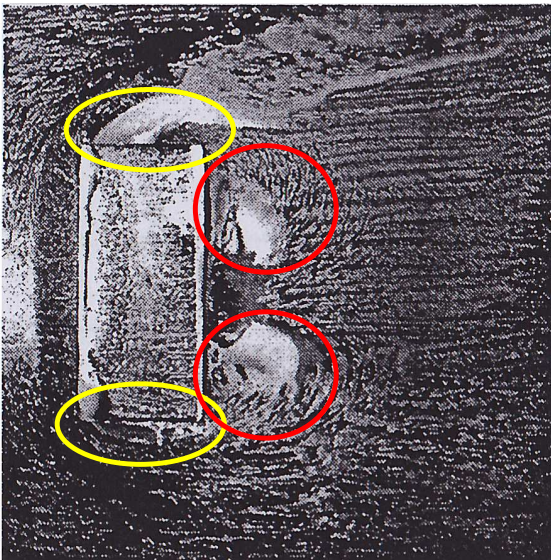

Fig. 17 Measured pathlines around the model building (from: [9]), top view (wind is coming from the left)
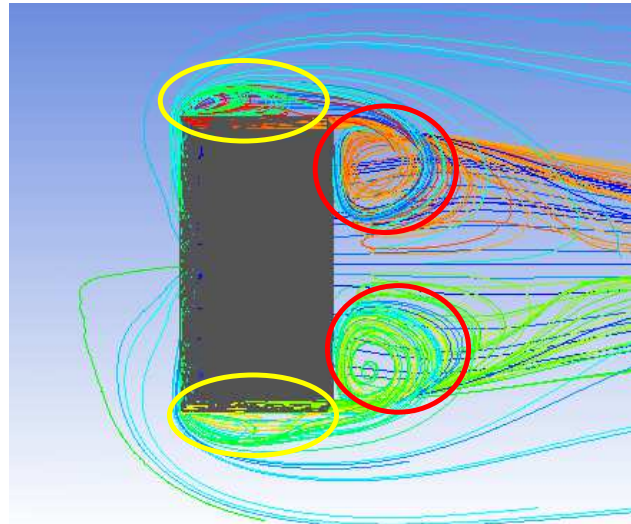

Fig. 18 Computed pathlines around the model building, top view (wind is coming from the left)

VII. CONCLUSIONS AND FUTURE WORKS

In the present work numerical validation tests have been performed against experimental atmospheric wind tunnel measurements, in order to develop some practical guidelines for CFD predictions of wind around buildings. An experimental case study [9] was chosen as the reference benchmark for the 3D numerical modeling of the flow around a simple rectangular building characterized by a flat roof.

The numerical code has proved to be accurate in predicting the main features of the flow field near the building model after the recirculation region in the upper portion of the model roof, while the prediction capabilities have lowered close to the upstream leading edge of the building model, in correspondence of the development of the separation bubble. A general underestimation of the experimental velocity measurements has been registered in the whole flow field. Further work is required in order to better investigate this phenomenon.

NOMENCLATURE

H [mm]	model height
$H_{wind\ tunnel}$ [mm]	wind tunnel test section height
I [-]	turbulence intensity
L_1 [mm]	distance between wind tunnel inlet condition and tested model
L [mm]	model length
$L_{wind\ tunnel}$ [mm]	wind tunnel length
Res_{domain} [-]	normalized grid resolution on outer computational domain
Res_{model} [-]	normalized grid resolution on the model building
u [m/s]	mean velocity along the horizontal axis
u' [m/s]	root-mean-square of the turbulent

velocity fluctuation

u_x' [m/s]   turbulent velocity fluctuation along the horizontal axis

U_0 [m/s]   reference velocity along the horizontal axis

W [mm]   model width

$W_{wind\ tunnel}$ [mm]   wind tunnel width

$x_{reference\ position}$ [mm]   distance between the scale model upstream leading edge and the reference position for the validation procedure

$\overline{x}$ [-]   normalized x-coordinate of the reference position for the validation procedure with respect to the model building length

y [mm]   coordinate along the vertical axis

δ [mm]   turbulent boundary layer thickness

δ/H [-]   ratio of boundary layer thickness to model height

Δg_{domain} [mm]   grid resolution on outer computational domain

Δg_{model} [mm]   grid resolution on the model building

REFERENCES

[1] T. Stathopoulos, "Wind Effects on People", *Proceedings of the International Conference on Urban Wind Engineering and Building Aerodynamics – Impact of Wind Storm on City Life and Built Environment*, COST Action C14, Von Karman Institute, Rode-Saint-Genèse (Belgium), 2004.

[2] P. Krishna, K. Kumar, N. M. Bhandari, IS:875 (Part3): *Wind Loads on Buildings and Structures – Proposed Draft & Commentary*, Document No. IITK-GSDMA-Wind02-V5.0 and IITK-GSDMA-Wind04-V3.0.

[3] N. M. Bhandari, P. Krishna, K. Kumar, A. Gupta, *An Explanatory Handbook on Proposed IS 875 (Part3) – Wind Loads on Buildings and Structures*, Document No. IITK-GSDMA-Wind06-V3.0.

[4] A. G. Jensen, J. Franke, C. Hirsch, M. Schatzmann, T. Stathopoulos, J. Wisse, N. G. Wright, *CFD Techniques – Computational Wind Engineering*, Proceedings of the International Conference on Urban Wind Engineering and Building Aerodynamics – Impact of Wind and Storm on City Life and Built Environment – Working Group 2, COST Action C14, Von Karman Institute, Rode-Saint-Genèse (Belgium).

[5] A. G. Jensen, J. Franke, C. Hirsch, M. Schatzmann, T. Stathopoulos, J. Wisse, N. G. Wright, *Impact of Wind and Storm on City Life and Built Environment – Working Group 2 – CFD Techniques – Computational Wind Engineering*, Proceedings of the International Conference on Urban Wind Engineering and Building Aerodynamics, COST Action C14, Von Karman Institute, Rhode-Saint-Genèse, Belgium, May 5-7, 2004.

[6] R. Yoshie, A. Mochida, Y. Tominaga, H. Kataoka, K. Harimoto, T. Nozu, T. Shirasawa, "Cooperative Project for CFD Prediction of Pedestrian Wind Environment in the Architectural Institute of Japan", *Journal of Wind Engineering and Industrial Aerodynamics*, 95 (2007) 1551-1578.

[7] J. Franke, C. Hirsch, A. G. Jensen, H. W. Krus, M. Schatzmann, P. S. Westbury, S. D. Miles, J. A. Wisse, N. G. Wright, "Recommendations on the Use of CFD in Wind Engineering", *Proceedings of the International Conference on Urban Wind Engineering and Building Aerodynamics*, COST Action C14, Von Karman Institute, Rhode-Saint-Genèse, Belgium, May 5-7, 2004.

[8] T. Stathopoulos, "Wind Effects on People", *Proceedings of the International Conference on Urban Wind Engineering and Building Aerodynamics*, COST Action C14, Von Karman Institute, Rhode-Saint-Genèse, Belgium, May 5-7, 2004.

[9] Y. Ozmen, J. P. A. J. Van Beeck, E. Baydar, "The Turbulent Flow over Three Dimensional Roof Modles Immersed in an Atmospheric Boundary Layer", *Proceedings of the International Conference on Urban Wind Engineering and Building Aerodynamics*, COST Action C14, Von Karman Institute, Rhode-Saint-Genèse, Belgium, May 5-7, 2004.

[10] M. Raciti Castelli, A. Castelli, E. Benini, "Modeling Strategy and Numerical Validation of the Turbulent Flow over a two-Dimensional Flat Roof", *World Academy of Science, Engineering and Technology*, Issue 79, July 2011, pp. 462-468.

[11] http://www.vki.ac.be/.

[12] B. Parmentier, R. Hoxey, J. M. Buchlin, P. Corieri, "The Assessment of Full Scale Experimental Methods for Measuring Wind Effects on Low Rise Buildings", *COST Action C14, Impact of Wind and Storm on City Life and Built Environment*, June 3-4, 2002, Nantes, France.

[13] J. Counihan, "An Improved Method of Simulating an Atmospheric Boundary Layer in a Wind Tunnel", *Atmos. Environ.*, Vol. 3 (1969), pp. 197-214.

[14] http://www.vki.ac.be/index.php?option=com_content&view=article&id=60:low-speed-wind-tunnel-l-2b&catid=48:low-speed-wind-tunnels&Itemid=151.